A New Coupled-Inductor Structure for Interleaving Bidirectional DC-DC Converters

Yugang Yang, *Member, IEEE*, Jie Ma, Carl N. M. Ho, *Senior Member, IEEE*, and Yufei Zou

***Abstract*—A new "EI∃" shape coupled inductor structure and its magnetic circuit models are presented. The proposed "EI∃" shape coupled inductor structure retains the advantages of high power density and tackles the drawback of high air gap fringing flux losses in conventional "E∃" shape coupled inductor structure. Besides, the proposed "EI∃" shape structure gives the advantages of shorter winding length and more uniform thermal distribution compared with the conventional "E∃" shape structure. The proposed "EI∃" shape structure and its magnetic models are successfully simulated by ANSYS and Maxwell2D, and implemented to apply to interleaving bidirectional DC/DC converter. Simulated and experimental results show that the proposed "EI∃" shape structure of coupled inductors is superior to the same volume "E∃" shape structure of coupled inductors in terms of temperature, inductance, losses, inductor ripple currents and efficiencies. The theoretical prediction and experimental results are in good agreement.**

***Index Terms*—Coupled inductors, magnetic core, interleaved technique, bidirectional DC/DC converter, air gap fringing flux.**

I. Introduction

In modern power electronic applications, interleaving bidirectional DC/DC converters are widely used in low power applications [1], Photovoltaic (PV) inverter applications [2]-[3], Fuel Cell (FC) applications [4], Uninterrupted Power Supply (UPS) applications [5], and Electric Vehicle (EV) applications [6] - [7], since this typically results of the lowest conduction loss and component cost. The Buck and Boost operating modes of a typical interleaving bidirectional DC/DC converter are shown in Fig. 1 [1] - [6]. There are at least two switching cells in one converter, and the two switching cells switch at 180° phase shift. This results small output ripple current (Buck converters) or input ripple current (Boost converters). Besides, the large current is shared by two cells, the thickness of copper windings is thinner. This leads to easier for manufacturing, and lower rated current class semiconductors can be used to have better semiconductor thermal management and higher switching frequency to reduce inductances [2].

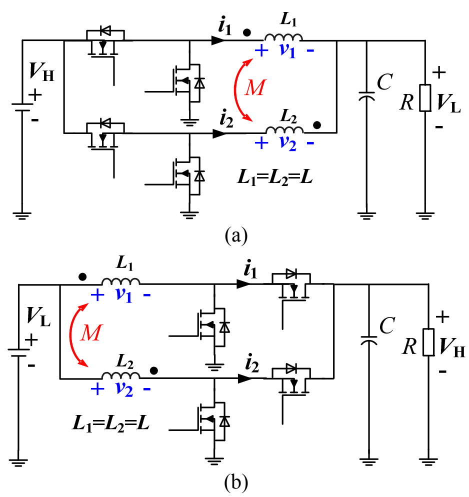

Fig. 1. Topology of 2-phase interleaving bidirectional DC/DC converter with coupled inductors: (a) Buck mode, (b) Boost mode.

Coupled inductors have been proposed for interleaved DC/DC converters to reduce the cost and increase the power density of magnetic components [8]. Typically, "EI" or "E∃" shape cores are used to form coupled inductors [1], [8] - [10]. The main advantage of using those two types of configuration is low bill of materials cost for converter manufacturing, this is because coupled inductors can be assembled by a piece of "E" shape core and a piece of "I" shape core, or two pieces of identical "E" shape cores and a wired bobbin. All components are commercial standard shapes and mass production products.

However, it is well known that the air gap should be minimized and separated from the coil in the inductors, since a large air gap generates extra power losses and a rise in the conductor temperature, which is caused by the air gap fringing flux [2] & [11]. From the converter point of view, it would reduce the system efficiency and reliability due to the high temperature.

Manuscript received May 4, 2015; accepted May 22, 2015. Date of publication June 08, 2015; date of current version June XX, 2015. The paper was presented in part at the *2014 IEEE International Power Electronics and Application Conference and Exposition*. The work was supported by the National Natural Science Foundation of China (51177067). Recommended for publication by Associate Editor XX XX.

Y. Yang, J. Ma, and Y. Zou are with the Department of Electrical & Control Engineering, Liaoning Technical University, Huludao (125105), Liaoning Province, China (e-mail: Yangyugang21@126.com).

C. N. M. Ho is with the Department of Electrical and Computer Engineering, University of Manitoba, Winnipeg, MB, R3T 5V6, Canada (e-mail: Carl.Ho@umanitoba.ca).

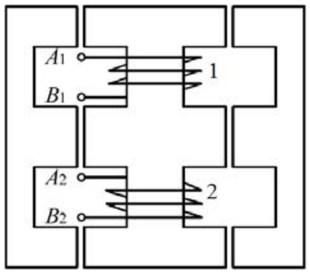

Fig. 2. Structure of proposed “EIƎ” shape coupled inductors.

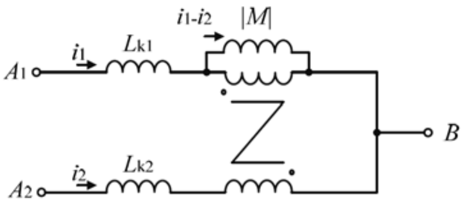

Fig. 3. Electrical circuit model of the proposed “EIƎ” shape coupled inductors.

A new “EIƎ” shape coupled inductor structure is proposed in this paper. It retains the benefit of the coupled inductors in high power density and tackles the drawback of the standard “EƎ” shape coupled inductors having high air gap fringing flux losses. Of particular importance, the thermal distribution of the proposed “EIƎ” shape structure is more uniformly distributed on the core, which is not concentrated on one or two spots. The structure of the proposed “EIƎ” shape coupled inductors and its magnetic circuit models will be given. The proposed “EIƎ” shape coupled inductors are successfully simulated by ANSYS and Maxwell2D, and implemented to apply to an interleaving bidirectional DC/DC converter. Simulated and experimental results show that the proposed “EIƎ” shape coupled inductors can have more uniform thermal distribution, lower losses, slightly higher inductances, smaller inductor ripple currents and higher efficiencies than the same volume of conventional “EƎ” shape coupled inductors. The theoretical prediction and experimental results are in good agreements.

II. The New Coupled Inductors

A. Structure of New Coupled Inductor

The structure of the proposed “EIƎ” shape coupled inductors is shown in Fig. 2. The magnetic core of the coupled inductors with “EIƎ” structure is formed by two pieces of “E” shape and one piece of “I” shape cores. The coils are wound on the “I” core in order to avoid the air gap fringing flux by separating the air gap and the coils.

B. Equivalent Electrical Circuit Model

Fig. 3 shows the equivalent electrical circuit model of the proposed “EIƎ” shape coupled inductors. It shows that the two-phase coupled inductors are symmetrical and inverse coupling, and the self-inductances of two windings are,

$$\begin{cases} L_1 = L_{k1} + |M| \\ L_2 = L_{k2} + |M| \end{cases} \quad (1)$$

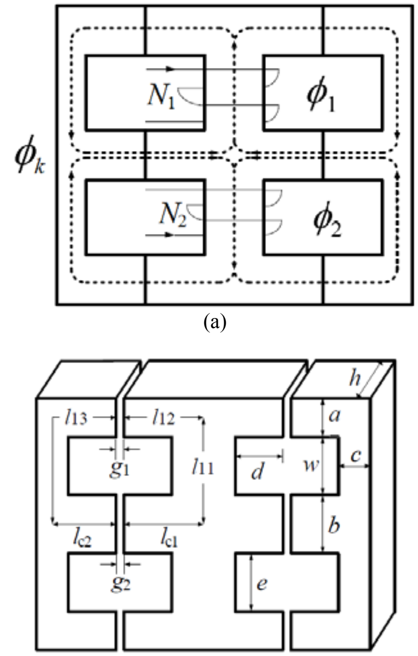

Fig. 4. Flux distribution and magnetic circuit length of the proposed coupled inductors: (a) Flux distribution, (b) Magnetic circuit length.

where L_1 and L_2 are the self-inductances of winding 1 and winding 2, respectively. L_{k1} and L_{k2} are the leakage inductances of winding 1 and winding 2, respectively. M is the mutual inductance between the two windings, and $M \leq 0$.

From the circuit point of view, the magnetic device characteristics are the same as that of the conventional coupled inductors such as in [9]-[12]. Ideally, the self-inductances, L_1 and L_2 are equal, thus they can be simplified as,

$$L_1 = L_2 = L \quad (2)$$

where L is the simplified inductance, and $-1 \leq M / L \leq 0$.

III. Magnetic Circuit Models and Characteristics

A. Basic Magnetic Circuit Models

The flux distribution of the new “EIƎ” shape coupled inductors is shown in Fig. 4(a). ϕ_1 are ϕ_2 are main fluxes of the 2 phase windings, ϕ_k is leakage flux, $N_1=N_2=N$ are the turn numbers of the windings. The magnetic circuit lengths of the flux are shown in Fig. 4 (b), a, b, c, d, e are the lengths of different core sections, g_1 and g_2 are the air gap lengths of outer legs and middle leg, respectively, l_{11}, l_{12}, l_{13}, l_{c1}, l_{c2} are magnetic circuit lengths, and h is the thickness of all the core sections.

The basic magnetic circuit model of the proposed coupled inductors is shown in Fig. 5 (a). According to Fig. 4 (a) and [10], the magnetic potential of the 2-phase windings can be described as,

$$\begin{cases} F_1 = N_1 i_1 \\ F_2 = N_2 i_2 \end{cases} \quad (3)$$

Besides, R_{11}, R_{12}, R_{13}, R_{c1}, R_{c2} are the core reluctances which are related to the corresponding core lengths. R_{g1} and R_{g2} are air

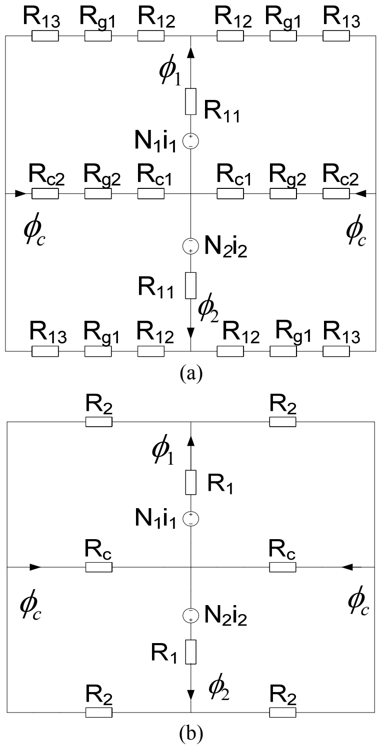

Fig. 5. Basic magnetic circuit model of the new coupled inductors: (a) Magnetic circuit model, (b) Basic Magnetic circuit model.

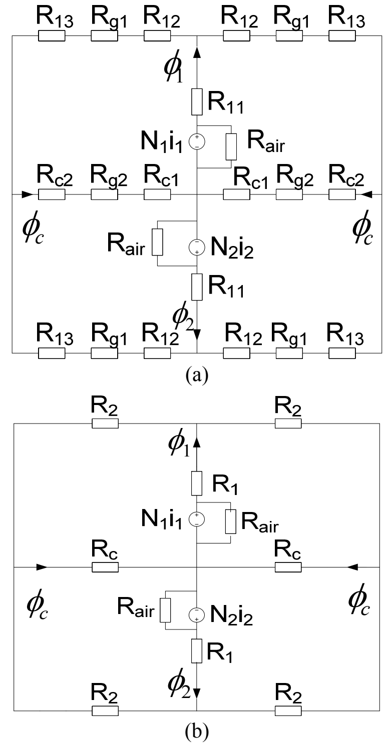

Fig. 6. Improved magnetic circuit model of the new coupled inductors: (a) Magnetic circuit model, (b) Improved Magnetic circuit model.

gap reluctances. By combining all parameters in a closed-loop magnetic circuit, the basic magnetic model is formulated and shown in Fig. 5 (b).

According to [13], the core reluctances R_{11}, R_{12}, R_{13}, R_{c1}, R_{c2} and air gap reluctances R_{g1} and R_{g2} in Fig. 5 (a) are determined by:

$$\begin{cases} R_{11} = \dfrac{1}{\mu_0 \mu_r} \dfrac{l_{11}}{2c \times h}, \quad R_{12} = \dfrac{1}{\mu_0 \mu_r} \dfrac{l_{12}}{a \times h} \\ R_{13} = \dfrac{1}{\mu_0 \mu_r} \dfrac{l_{13}}{a \times h}, \quad R_{c1} = \dfrac{1}{\mu_0 \mu_r} \dfrac{l_{c1}}{b \times h} \\ R_{c2} = \dfrac{1}{\mu_0 \mu_r} \dfrac{l_{c2}}{b \times h} \end{cases} \tag{4}$$

$$\begin{cases} R_{g1} = \dfrac{1}{\mu_0} \dfrac{g_1}{a \times h} \\ R_{g2} = \dfrac{1}{\mu_0} \dfrac{g_2}{b \times h} \end{cases} \tag{5}$$

where μ_0 is the permeability of free space (air), μ_r is the relative material permeability of core. The reluctances R_1, R_2 and R_c in Fig. 5 (b) can be expressed as:

$$\begin{cases} R_1 = R_{11} \\ R_2 = R_{12} + R_{g1} + R_{13} \\ R_c = R_{c1} + R_{g2} + R_{c2} \end{cases} \tag{6}$$

Therefore, the self-inductances and the leakage inductances of the proposed coupled inductors in Fig. 2 are:

$$L_1 = L_2 = \frac{N^2 (2R_c + 2R_2 + 4R_1)}{(2R_1 + R_2)(2R_1 + R_2 + 2R_c)} \tag{7}$$

$$L_{k1} = L_{k2} = \frac{2N^2}{2R_1 + R_2 + 2R_c} \tag{8}$$

B. Improved Magnetic Circuit Models

In order to increase the accuracy of the basic magnetic model in Fig. 5, the edge effect of air gap magnetic field and the air leakage flux outside the windings have to be considered. The improved magnetic circuit model of the proposed coupled inductors is based on Fig. 5 (a) and which is shown in Fig. 6 (a). The edge effect of magnetic fields in air gaps, g_1 and g_2, are considered in the air gap reluctances, R_{g1} and R_{g2}, and the magnetic potentials, $N_1 i_1$ and $N_2 i_2$, are paralleled with air reluctances R_{air1} and R_{air2}, respectively.

1) Air gap reluctances

Based on the improved magnetic circuit model and [11], the outer legs air gap reluctance R'_{g1} and the middle leg air gap reluctance R'_{g2} are:

$$\begin{cases} R'_{g1} = \dfrac{1}{\mu_0 h \left[\dfrac{a}{g_1} + \dfrac{2}{\pi} \left(1 + \ln \dfrac{\pi d}{2 g_1} \right) \right]} \\ R'_{g2} = \dfrac{1}{\mu_0 h \left[\dfrac{b}{g_2} + \dfrac{2}{\pi} \left(1 + \ln \dfrac{\pi d}{2 g_2} \right) \right]} \end{cases} \tag{9}$$

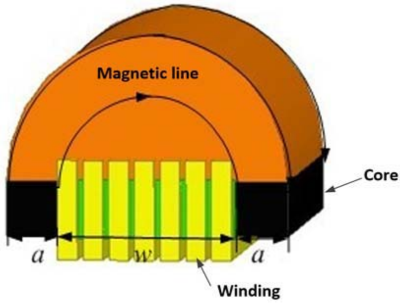

Fig. 7. The magnetic line outside the winding.

where d is defined in Fig. 4, which is the length of core leg and it can be designed by,

$$d=N'd_1+2\delta \tag{10}$$

where N' is layer number of winding, d_1 is thickness of each winding layer, δ is the sum of margin between the winding and its window.

2) Air reluctance outside the windings

According to [14], there are magnetic fields outside the windings. Fig. 7 shows a simplified diagram to indicate the magnetic line of force distribution around the winding which is wound on the high side of "Ɨ" core. The complete air region of magnetic lines of force of the proposed coupled inductors is shown in Fig. 8. According to the diagram, it can be divided into two parts of passing the magnetic line of force, which are front part, the reluctance of the front part is R_t, and back part, the reluctance of the back part is R_b. The air reluctances of the two-phase windings are:

$$R_{air1}= R_{air2}= R_t \parallel R_b \tag{11}$$

Assume the front side and back side turns are identical, the reluctances R_t and R_b can be determined by,

$$R_b=R_t \approx \frac{\bar{l}}{\mu_0 \bar{S}_t} \tag{12}$$

where $\bar{l}$ is the average magnetic line length of the reluctance region,

$$\bar{l}=\frac{l_{min}+l_{max}}{2} \tag{13}$$

and
$$\begin{cases} l_{min}=w \\ l_{max}=\dfrac{\pi(w+2a)}{2} \end{cases} \tag{14}$$

where $\bar{S}_t$ is the average cross section area of the reluctance region. It can be estimated by the volume of the reluctance region, V_t, divided by the average magnetic line length. If the shape of the magnetic field is considered as a half cylinder in Fig. 8, $\bar{S}_t$ can be determined by,

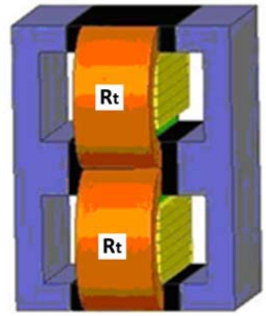

Fig. 8. Air reluctance outside the windings of the proposed coupled inductors.

$$\bar{S}_t=\frac{V_t}{\bar{l}}=\frac{\pi h\left(\frac{w}{2}+a\right)^2}{2\bar{l}} \tag{15}$$

3) Inductance of the improved magnetic circuit model

The self-inductances L_1, L_2 and the leakage inductances L_{k1}, L_{k2} of the improved magnetic circuit model in Fig. 6 can be determined as:

$$L_1=L_2=\frac{2N^2(R_c+R_2+2R_1)}{(2R_1+R_2)(2R_1+R_2+2R_c)}+\frac{N^2}{R_{air}} \tag{16}$$

$$L_{k1}=L_{k2}=\frac{2N^2}{2R_1+R_2+2R_c}+\frac{N^2}{R_{air}} \tag{17}$$

IV. SIMPLIFIED DESIGN PROCEDURES

The values of $L_1=L_2=L$, $L_{k1}=L_{k2}=L_k$ and the core size of the proposed "EƗƎ" structure coupled inductors are designed by the following procedures.

A. *System Characteristics*

In buck mode of the interleaving bidirectional DC/DC converter as shown in Fig. 1 (a), the steady state output ripple current peak to peak value is ΔI_o, the duty cycle increase is ΔD, the transient inductor current increase at ΔD is Δi, the transient inductor current response speed is $\Delta i/\Delta D$, $\Delta i/\Delta D$ can be described by [10],

$$\frac{\Delta i}{\Delta D}=\frac{V_{in}}{L\cdot f_S} \tag{18}$$

where V_{in} is the input voltage, f_s is the switching frequency.

B. *Determination of Self-inductance and Leakage Inductance*

When bidirectional DC/DC converter is designed, the specification of $\Delta i/\Delta D$ needs to be guaranteed as the specifications of ΔI_o and $\Delta i/\Delta D$ cannot be met simultaneously. In order to meet the specification of $\Delta i/\Delta D$, the leakage inductance L_k is:

$$L_k=\frac{2V_{in}}{f_s}\cdot\frac{\Delta D}{\Delta i} \tag{19}$$

TABLE I
"E" SHAPE CORE DIMENSIONS

a	b	c	d	E	h
3mm	6mm	3mm	3mm	10mm	20mm

TABLE II
INDUCTANCE OF "EIƎ" AND "EE" COUPLED INDUCTORS

Self inductance(uH)		Mutual inductance(uH)	
Proposed EIƎ	Conventional EƎ	Proposed EIƎ	Conventional EƎ
36.8	31.2	-13.2	-8.7

In order to meet the specification of output current ripple peak to peak value, ΔI_o, the designed steady state ripple current, $\Delta I'_o$ is:

$$\Delta I_o^{'} = \frac{1-2D}{L_k} \cdot \frac{V_o}{f_s} \tag{20}$$

$\Delta I'_o$ should smaller than ΔI_o, Where V_o is the output voltage.

If $\Delta I'_o \leq \Delta I_o$, it means that the design is reasonable, the demand of steady state ripple current specification can be met. Otherwise, if $\Delta I'_o > \Delta I_o$, it means that the designed coupled inductors can meet the specification of transient current response speed $\Delta i/\Delta D$, but can not meet the specification of steady state ripple current ΔI_o. The self-inductance L is:

$$L = \frac{L_k}{1+k} \tag{21}$$

where k is coupling coefficient, and $-1 \leq k \leq 0$.

C. Determination of Core Size

The maximum flux density of central core middle pole is:

$$B_{\max} = \left[L_k \cdot \frac{I_o}{2} + \frac{V_o(1\text{-}2D)}{f} \right] / A \leq B_{sat} \tag{22}$$

Where A is cross section area of the central core, B_{sat} is saturation flux density of core material. The value of A can be obtained with equation (22), the values of a, b, c, h can be obtained with $A=b\times h$, $b=2\times a$ and $c=a$, as shown in Fig. 4(b). The air gap lengths g_1 and g_2 can be obtained by substituting the inductance values calculated with equations (19) and (21) into equations (16) and (17), and $l_{c2} = \frac{2d + g_1 - g_2}{2}$

V. SIMULATION

A. Structure of the proposed "EIƎ" shape Coupled inductors

The proposed "EIƎ" shape coupled inductors is designed according to the simplified design procedures and it is built with four pieces of "E" cores with back to back configuration. The size of "E" core is shown in Table I. In order to verify the claimed advantages of the proposed "EIƎ" shape coupled inductors comparing to conventional "EƎ" shape coupled inductors, a standard "EƎ" shape coupled inductors are designed with two pairs of "E" cores in parallel, which is same as the "E" core constituting the proposed "EIƎ" shape coupled inductors. It is noticed that the overall volume of both the "EIƎ" shape and "EƎ" shape cores are the same. The corresponding physical meaning of the parameters in Table I are shown in Fig. 4, where h is the thickness of core. The winding space of the proposed "EIƎ" shape core is $2a\times h$, thus, "EIƎ" core's middle pole perimeter is $2(2a+h)$=52mm. On the other hand, the winding space of standard "EE" shape core is $a\times 2h$, thus, "EE" core's side pole perimeter is $2(a+2h)$=86mm. According to the numbers of 52mm and 86mm, it can be seen that the winding length of the proposed "EIƎ" shape core is shorter than that of the standard "EƎ" shape core. In other words, the proposed "EIƎ" shape core shortens the length of each winding turn by 40% (34mm). This pronominally reduces copper material cost and copper loss.

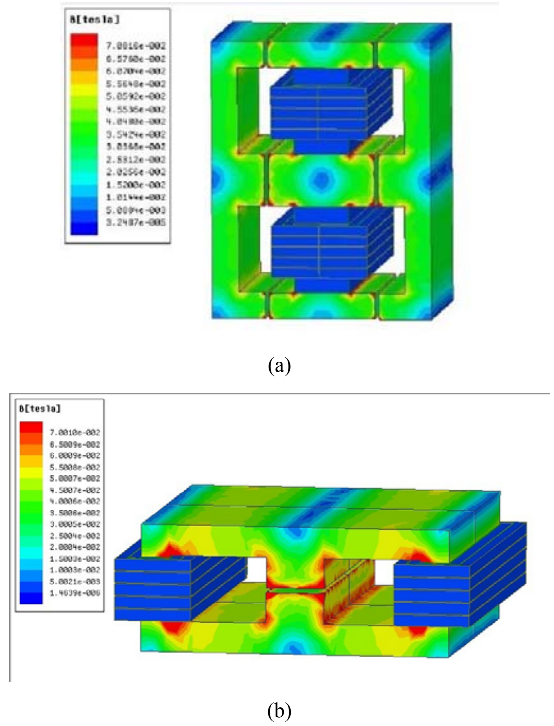

Fig. 9. Flux density simulation of (a) the proposed coupled inductors, and (b) the conventional coupled inductors.

B. Inductances

In order to have a comparative study of the proposed "EIƎ" and the conventional "EƎ" coupled inductors. Both inductor models have been created and simulated with ANSYS simulator. The turns number and air gap length are the same in both structures, which are all 10 turns and 0.45mm, respectively. Table II shows the simulated self-inductance and mutual inductance of both inductors. It can be seen that the proposed "EIƎ" inductor structure is larger than the conventional "EƎ" inductor structure in both inductances with the same core volume, core cross section area, air gap length and winding turn number.

C. Simulation of Core Flux Density

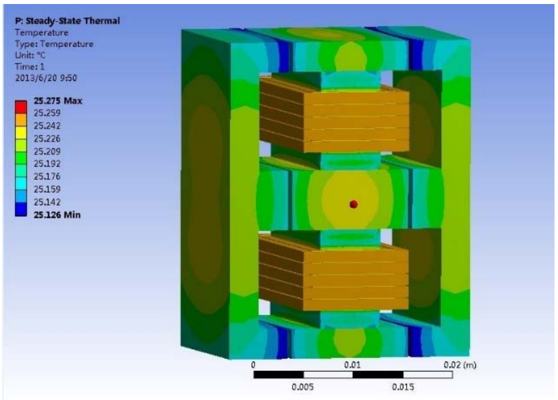

(a)

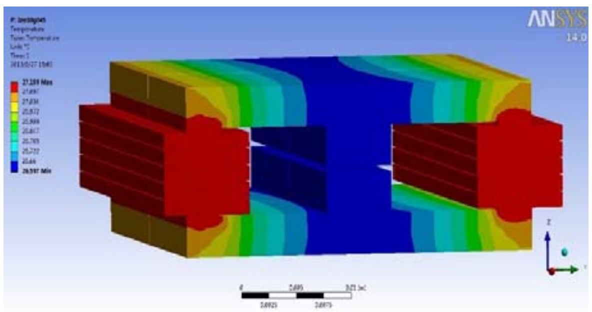

(b)

Fig. 10. Temperature performance simulation of (a) the proposed coupled inductors, and (b) the conventional coupled inductors.

The core flux densities of the proposed and conventional inductors are simulated with ANSYS simulator by supplying 3A current as shown in Fig. 9 (a) and (b), respectively. The simulation results show that the maximum flux densities of the two inductors are the same.

D. Simulation of Thermal Performance

The thermal performance of the proposed and conventional inductors are simulated with ANSYS simulator by supplying 3A current as shown in Fig. 10 (a) and (b), respectively. The steady-state temperature of the proposed coupled inductors is in the range of 25.126~25.275℃, however, that of the conventional coupled inductors is in the range of 26.597~27.159℃. The resultant temperature of the proposed coupled inductors is lower than that of the conventional coupled inductors.

E. Simulation of flux distribution

The flux distribution of the proposed and conventional inductors are simulated with Maxwell 2D simulator by supplying 3A current as shown in Fig. 11 (a) and (b). The flux consists of three parts: (1) The main flux; (2) The diffusion flux that permeates the window near the air gap; (3) The bypass flux that passes through the window between the core poles. The simulation results show that the diffusion flux and the bypass flux of the proposed "EIƎ" shape coupled inductor are much smaller than those of the conventional "EƎ" shape coupled inductors. It is because the windings of the proposed coupled inductors are far away from the air gaps.

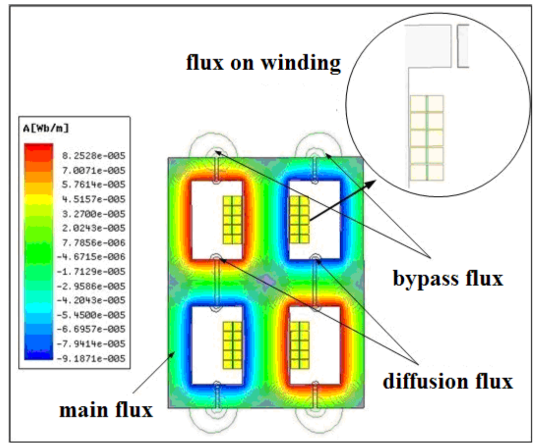

(a)

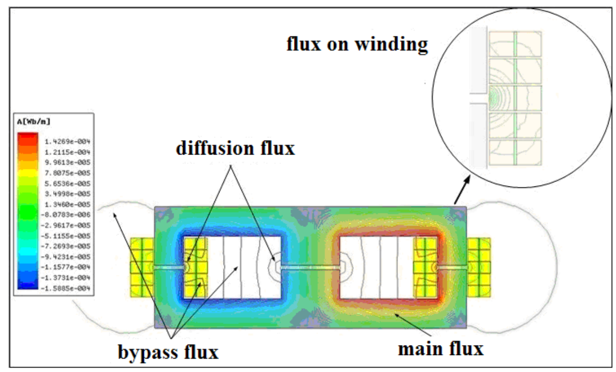

(b)

Fig. 11. Magnetic line of force in (a) the proposed coupled inductors, and (b) the conventional coupled inductors.

VI. EXPERIMENTAL VERIFICATIONS

A. Implementation of Coupled inductors

As well as the simulated inductor structures, both coupled inductors are formed by same four pieces of "E"-core with the dimensions in Table I. The turn number of windings is 10 turns, and the length of air gaps is 0.45mm. Fig. 12 shows the prototypes of the two inductor configurations. The self-inductance and mutual inductance have been measured a transformer test system. Table III shows the measured results and comparing with the results calculated with the magnetic circuit models and the ANSYS simulations. It can be seen that, 1) the measured results are very close to the simulated results, and 2) the improved magnetic circuit model has a higher accuracy than the based magnetic circuit model for designing the proposed coupled inductors. In contrast, the conventional "EƎ" coupled inductors have been measured also. Table IV shows the difference of self-inductance and mutual inductance of the conventional coupled inductance between simulations and measurements. It shows that the errors are relatively small and the proposed coupled inductors have higher inductance than the conventional coupled inductors in both self-inductance and mutual inductance in measurements.

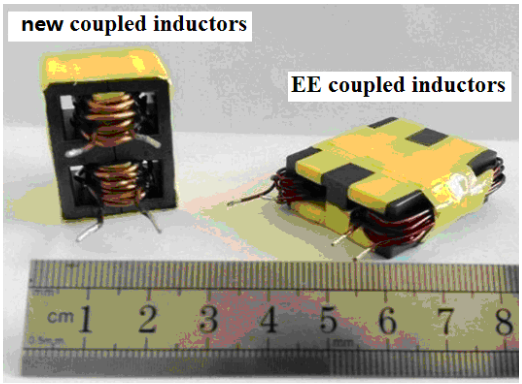

Fig. 12. Prototypes of the proposed and conventional coupled inductors.

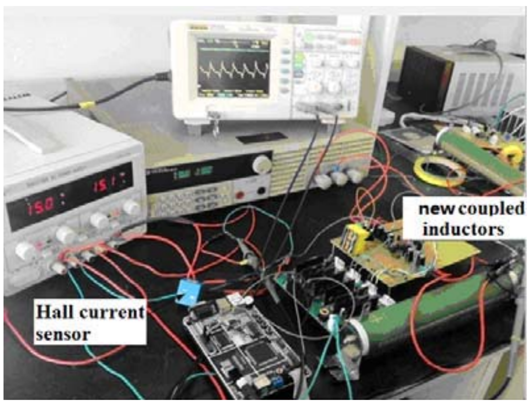

Fig. 13. Photograph of the prototype and the measuring setup.

B. Evaluation of Interleaving Bidirectional DC/DC Converters with the proposed "EIƎ" coupled inductors

The interleaving bidirectional DC/DC converters as shown in Fig. 1 are evaluated by using the proposed "EIƎ" coupled inductors. The prototype and the measuring setup are shown in Fig. 13. Basically, the converters can be considered as one topology consisting of two operating modes, Buck mode and Boost mode. Table V lists the specifications and operating conditions of two operating modes.

At the same specifications and operating conditions as shown in Table V, Fig. 14 (a) shows the measured output voltage of the converter and the current waveform of the proposed "EIƎ" coupled inductors in Buck mode. Meanwhile Fig. 14 (b) shows the measured output voltage of the converter and the current waveform of the conventional "EƎ" coupled inductors in the Buck mode. Fig. 14 (a) shows the ripple current peak to peak value of the proposed "EIƎ" coupled inductors is 0.38A, which is smaller than that of the conventional "EƎ" coupled inductors, 0.4A, as shown in Fig. 14 (b), the decrease is (0.4-0.38)/0.4=5.0%.

At the same specifications and operating conditions as shown in Table V, Fig. 15 (a) shows the measured output voltage of the converter and the current waveform of the proposed "EIƎ" coupled inductors in Boost mode. Meanwhile Fig. 15 (b) shows the measured output voltage of the converter and the current waveform of the conventional "EƎ" coupled inductors in the Boost mode. Fig. 15 (a) shows the ripple current peak to peak value of the proposed "EIƎ" coupled inductors is 0.42A, which is smaller than that of the conventional "EƎ" coupled inductors, 0.45A, as shown in Fig. 15 (b), the decrease is (0.45-0.42)/0.45=6.7%.

TABLE III
INDUCTANCES OF THE PROPOSED "EIƎ" COUPLED INDUCTOR

Inductance		Self-Inductance	Mutual Inductance
Basic magnetic circuit model	Inductance(uH)	32.05	-12.4
	Error	11.7%	6.8%
Improved magnetic circuit model	Inductance(uH)	33.6	-12.7
	Error	7.4%	4.5%
ANSYS simulation	Inductance(uH)	36.8	-13.2
	Error	1.38%	0.8%
Experiment Measurement		36.3	-13.3

TABLE IV
INDUCTANCES OF THE CONVENTIONAL "EE" COUPLED INDUCTOR

Inductance		Self-Inductance	Mutual Inductance
ANSYS simulation	Inductance(uH)	31.2	-8.7
	Error	3.0%	4.8%
Experiment Measurement		30.3	-8.3

TABLE V
SPECIFICATIONS OF THE DC-DC CONVERTERS

Operating modes & Structures of coupled inductors	Buck Mode		Boost Mode	
	EIƎ	EƎ	EIƎ	EƎ
Input Voltage: V_H/V_L	10V	10V	10V	10V
Output Voltage: V_L/V_H	2.0V	2.0V	14.0V	14.0V
Switching Frequency: f_s	100kHz	100kHz	100kHz	100kHz
Duty Ratio: D	0.2	0.2	0.32	0.32
Load Resistance: R	0.8Ω	0.8Ω	9.33Ω	9.33Ω
Output Current: I_O	2.5A	2.5A	1.5A	1.5A

C. Efficiency of Interleaving Bidirectional DC/DC Converters with the proposed "EIƎ" coupled inductors

At the same specifications and operating conditions as shown in Table V, Fig. 16 (a) shows the measured efficiencies of the converter in Buck mode with the proposed "EIƎ" new coupled inductors and the conventional "EƎ" coupled inductors. The efficiency of the proposed "EIƎ" new coupled inductors is higher than that of the conventional "EƎ" coupled inductors. The max increase is 1.4%.

At the same specifications and operating conditions as shown in Table V, Fig. 16 (b) shows the measured efficiencies of the converter in Boost mode with the proposed "EIƎ" coupled inductors and the conventional "EƎ" coupled inductors. The efficiency of the proposed "EIƎ" coupled inductors is higher than that of the conventional "EƎ" coupled inductors. The max increase is 1.0%.

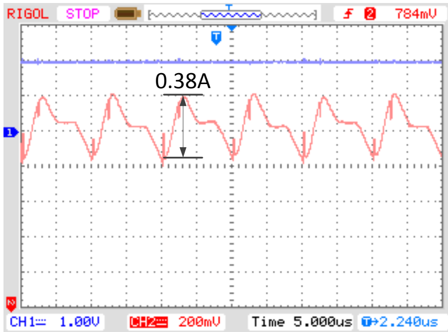

(a)

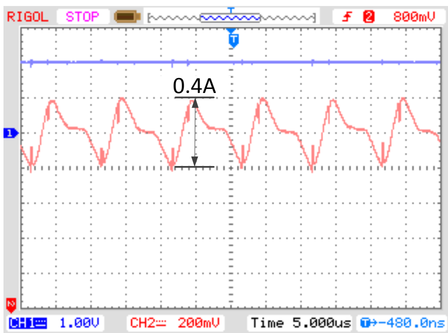

(b)

Fig. 14. Measured output voltage and inductor current waveforms of (a) the proposed “EIƎ” and (b) the conventional “EƎ” coupled inductors applied in Buck mode of bidirectional DC/DC converter with the output voltage, 2V, and output current, 2.5A.

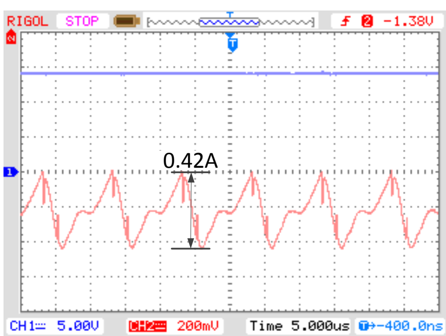

(a)

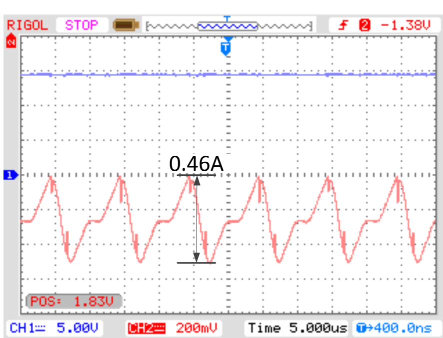

(b)

Fig. 15. Measured output voltage and inductor current waveforms of (a) the proposed “EIƎ” and (b) the conventional “EƎ” coupled inductors applied in Boost mode of bidirectional DC/DC converter with the output voltage, 14.0V, and output current, 1.5A.

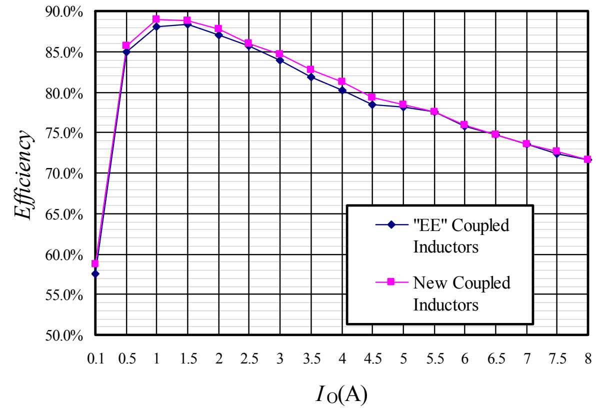

(a)

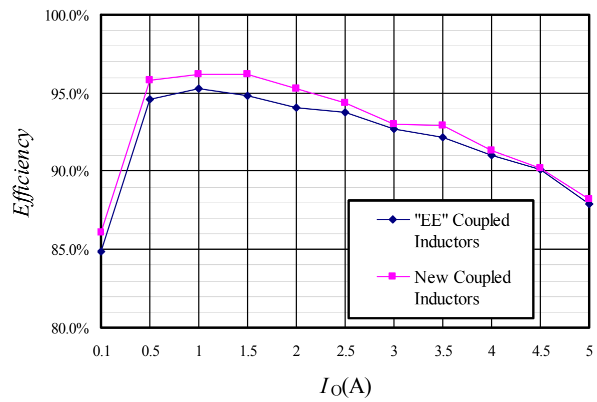

(b)

Fig. 16. Measured efficiencies of interleaving bidirectional DC/DC converter with the proposed “EIƎ” new coupled inductors and conventional “EƎ” coupled inductors: (a) Buck mode (10V/2V), (b) Boost mode (10V/14V)

VII. Conclusion

This paper has presented a new core structure for coupled inductors. The core is assembled by “EIƎ” shapes core and the two coils are wound on the middle leg. This leads to reduce the length of the wires to reduce the copper material cost and conduction loss. And it effectively reduces the loss which is caused by the air gap fringing flux by separating air gap and coils. Besides, the temperature distribution is more uniform on the core. It can improve reliability of the inductors. Moreover, the magnetic circuit models were derived to improve the prediction accuracy. The proposed “EIƎ” coupled inductors have been verified and compared with the conventional “EƎ” inductors by simulations and with an interleaving bidirectional DC/DC converter. The performances of the proposed “EIƎ” coupled inductors have been demonstrated. Experimental measurements are favorably verified with simulation and theoretical results. The Experimental measurements show that the proposed “EIƎ” shape coupled inductors can decrease inductor ripple currents and increase efficiency when they are used in interleaving bidirectional DC/DC converter.

References

[1] X. Zhou, P.L. Wong, P. Xu, and F.C. Lee, "Investigation of candidate VRM topologies for future microprocessors", *IEEE Transactions on Power Electronics*, Vol. 15, No. 6, pp. 1172 – 1182, Nov. 2000.

[2] C. Ho, H. Breuninger, S. Pettersson, G. Escobar, L. Serpa, and A. Coccia, "Practical design and implementation procedure of an interleaved boost converter using SiC diodes for PV applications", *IEEE Transactions on Power Electronics*, vol. 27, no. 6, Jun. 2012, pp. 2835 - 2845.

[3] C. Ho, H. Breuninger, S. Pettersson, G. Escobar and F. Canales, "A comparative performance study of an interleaved boost converter using commercial Si and SiC diodes for PV applications", *IEEE Transactions on Power Electronics*, vol. 28, no. 1, Jan. 2013, pp. 289 - 299.

[4] O. Hegazy, J. Van Mierlo, and P. Lataire, "Analysis, modeling, and implementation of a multidevice interleaved DC/DC converter for fuel cell hybrid electric vehicles", *IEEE Transactions on Power Electronics*, Vol. 27, No. 11, pp. 4445 – 4458, Nov. 2012.

[5] F. Forest, T.A. Meynard, E. Labouré, V. Costan, E. Sarraute, A. Cuniere, and T. Martire, "Optimization of the Supply Voltage System in Interleaved Converters Using Intercell Transformers", *IEEE Transactions on Power Electronics*, Vol. 22, No. 3, pp. 934 – 942, May. 2007.

[6] F. Musavi, W. Eberle, W.G. Dunford "A high-performance single-phase bridgeless interleaved PFC converter for plug-in hybrid electric vehicle battery chargers", *IEEE Transactions on Industry Applications*, Vol. 47, No. 4, pp. 1833 – 1843, Jul./Aug. 2011.

[7] O. García, P. Zumel, A. de Castro, and J. A. Cobos, "Automotive DC–DC Bidirectional Converter Made With Many Interleaved Buck Stages". *IEEE Transactions on Power Electronics*, Vol. 21, No. 3, pp. 578 – 586, May 2006.

[8] US4384321A "Unity Power Factor Switching Regulator", US Patents, 17 May 1983.

[9] F. Yang, X. Ruan, Y. Yang and Z. Ye, "Interleaved critical current mode boost PFC converter with coupled inductor", *IEEE Transactions on Power Electronics*, Vol. 26, No. 9, pp. 2404 – 2413, Sept. 2011.

[10] P.-L. Wong, P. Xu, B. Yang, and F.C. Lee, "Performance improvements of interleaving VRMs with coupling inductors", *IEEE Transactions on Power Electronics*, Vol. 16, No. 4, pp. 499 – 507, July. 2001.

[11] J. Fletcher, B. Williams, and M. Mahmoud, "Airgap fringing flux reduction in inductors using open-circuit copper screens," *IEE Proc.-Electr. Power Appl.*, vol. 152, no. 4, p. 990-996, Jul. 2005.

[12] P.-W. Lee, Y.-S. Lee, D. Cheng, and X.-C. Liu, "Steady-state analysis of an interleaved boost converter with coupled inductors", *IEEE Transactions on Industrial Electronics*, Vol. 47, No. 4, pp. 787 – 795, Aug. 2000.

[13] A. Balakrishnan, W.T. Joines, and T.G. Wilson, "Air-gap reluctance and inductance calculations for magnetic circuits using a Schwarz- Christoffel transformation," *IEEE Transactions on Power Electronics*, Vol. 12, No. 4, pp. 654 – 663, July. 1997.

[14] A. Hoke, and C. R. Sullivan, "An improved two-dimensional numerical modeling method for E-core transformers", *the IEEE Applied Power Electronics Conference*, Dallas, US, 2002.

Yugang Yang (M'14) received the B.S. and M.S. degrees in electrical engineering from Fuxin Mining College, Fuxin, China, in 1989 and 1993, and the Ph.D. degree in electrical engineering from Tsinghua University, Beijing, China, in 1997.

From 1998 to 2001, he was a Senior Engineer of power electronics at Huawei Company, Shenzhen, China. From Sep. 2004 to Dec. 2004, he was a Visiting Scholar at Technical University of Clausthal, Clausthal, Germany. From Jan. 2006 to Jan. 2007, he was a Visiting Scholar at Virginia Polytechnic Institute and State University, Blacksburg, USA. From Jan. 2013 to July 2013, he was a Visiting Scholar at Florida State University, Tallahassee, USA.

Dr. Yang is currently a Professor at Liaoning Technical University, Huludao, China. Since 2001, he has been teaching and conducting research on magnetic components and their integration in power electronics converters at Liaoning Technical University. His main research interests include magnetic integration in power electronics converters and bidirectional DC/DC converters.

Jie Ma was born in Hebei, China, in 1988. He received the B.S. degree in electric power system and automation from the Liaoning Technical University.

He is curretly pursuing the M.S. degree in Power electronics and motor drive at the electrical and control engineering Institution, Liaoning Technical University, China. His research interests include dc-dc converters, coupled inductors, and soft-switching techniques.

Carl Ngai-Man Ho (M'07, SM'12) received the B.Eng. and M.Eng. double degrees and the Ph.D. degree in electronic engineering from the City University of Hong Kong, Kowloon, Hong Kong, in 2002 and 2007, respectively. His Ph.D. research was focused on the development of dynamic voltage regulation and restoration technology.

From 2002 to 2003, he was a Research Assistant at the City University of Hong Kong. From 2003 to 2005, he was an Engineer at e.Energy Technology Ltd., Hong Kong. . In 2007, he joined ABB Switzerland. He has been appointed as Scientist, Principal Scientist, Global Intellectual Property Coordinator and the last position was R&D Principal Engineer. He has led a research project team at ABB for three years to develop Solar Inverter technologies. In October 2014, he joined the University of Manitoba in Canada as Assistant Professor and Canada Research Chair in Efficient Utilization of Electric Power. He takes up the challenge of research into Microgrid technologies, Renewable Energy interfaces and demand side control methodologies.

Dr. Ho is currently an Associate Editor of the IEEE Transactions on Power Electronics and Guest Associate Editor of the IEEE Journal of Emerging and Selected Topics in Power Electronics – Special Issue on Sustainable Energy Systems Integration.

Yufei Zou was born in Shenyang, China, in 1991. She received the B.S. degree in automation specialty from the Liaoning Technical University. She is currently pursuing the M.S. degree in control theory and control engineering, Liaoning Technical University, China. Her research interests include dc-dc converters, coupled inductors, and soft-switching techniques.